ACS Macro Letters

Letter

pubs.acs.org/macroletters

Use of Ion Mobility Spectrometry–Mass Spectrometry to Elucidate Architectural Dispersity within Star Polymers

Casey D. Foley,[†] Boyu Zhang,[‡] Alina M. Alb,[§] Sarah Trimpin,*[,†] and Scott M. Grayson*[,‡]

[†]Department of Chemistry, Wayne State University, 5101 Cass Avenue, Detroit, Michigan 48202, United States

[‡]Department of Chemistry and [§]Department of Physics, Tulane University, New Orleans, Louisiana 70118, United States

Supporting Information

ABSTRACT: The power of ion mobility spectrometry–mass spectrometry (IMS-MS) as an analytical technology for differentiating macromolecular architecture is demonstrated. The presence of architectural dispersity within a sample is probed by sequentially measuring both the drift time and the mass-to-charge ratio for every component within a polymer sample. The utility of this technology is demonstrated by investigating three poly(ethylene glycol) (PEG) architectures with closely related average molecular weights of about 9000 Da: a linear PEG, an unevenly branched miktoarm star PEG, and evenly branched homoarm star PEGs. The three architectures were readily distinguished when analyzed separately as "pure" architectures or when analyzed as mixtures. IMS-MS results are contrasted with matrix-assisted laser desorption/ionization-MS and viscometry measurements.

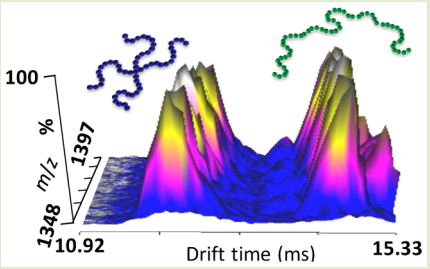

The molecular architecture of polymers has a profound effect on their physical properties and therefore their potential applications. In the case of star polymers, the multiplicity of end groups and more globular shape relative to linear polymers imparts on them a set of unique physical properties.[1−5] Traditionally, star polymers are most easily prepared via a divergent growth technique, in which the polymer arms are grown outward from a central core.[6−8] While it might be assumed that each arm generated by this technique should have a similar degree of polymerization, steric hindrance from neighboring arms can result in failed initiation or truncated arms.[9] However, despite this concern about structural inhomogeneity, there is no simple screening method for rapidly determining the purity of star polymers with regards to dispersity in arm number or length. To avoid these architectural impurities, many convergent approaches have been developed to prepare well-defined star polymers, including reaction of preformed linear arms with a multifunctional core using highly efficient coupling reactions.[10,11] While this convergent route ensures the uniformity of the arms within a star polymer, it requires much more effort during synthesis and purification (e.g., removal of excess arms).[12,13] Without any analytical technology capable of determining structural irregularities within star polymer samples, it can be difficult to justify the additional effort required by convergent routes.

Classic small-molecule characterization technology, such as nuclear magnetic resonance (NMR), is limited in its ability to identify structural dispersity because the signal of the polymer backbone often overwhelms that of the end groups or branching points, making relative quantification unreliable. As a result, these methods are often incapable of differentiating between stars with the same molecular weight (MW) but dissimilar arm numbers or lengths.

While technologies such as viscometry and light scattering are useful in determining aspects of polymer size and shape,[14,15] they measure the average properties of an entire polymer sample and therefore cannot measure architectural dispersity within a sample. Techniques like size exclusion chromatography (SEC) can determine distributions with respect to hydrodynamic radius[16,17] but cannot directly differentiate polymer architecture within such distributions. Finally, mass spectrometry (MS) can provide exceptional resolution of polymer mass distributions, easily resolving every individual *n*-mer unit of a homopolymer by its mass-to-charge (m/z) ratio.[18] In addition, ultrahigh resolution MS combined with tandem MS can also give clues to copolymer composition where conventional matrix-assisted laser desorption/ionization (MALDI) time-of-flight (TOF) has difficulties.[19−22] However, irrespective of the highest mass resolution, MS alone cannot differentiate isomeric molecular architectures.[23,24]

Ion mobility spectrometry (IMS) coupled with MS may offer the exceptional ability to detect architectural dispersity within a polymer sample.[25] For biomacromolecules, the ability of IMS-MS to differentiate biopolymers by shape has been used to distinguish between the native folded state of a protein and its intact but denatured analogue.[26,27] The applicability of IMS-MS for the structural characterization of synthetic polymers was first demonstrated by distinguishing between skeletal isomers (*n*-Bu versus *t*-Bu) of poly(butyl methacrylate)[23] and by differentiating between linear and cyclic poly(ε-caprolactone).[28] IMS-MS has also been used to confirm the cyclic structure of polypeptoids[29] and poly(lactide),[30] to discern poly(ε-capro-

Received: May 4, 2015
Accepted: July 1, 2015
Published: July 7, 2015

DOI: 10.1021/acsmacrolett.5b00299
ACS Macro Lett. 2015, 4, 778−782

lactone) stars with differing numbers of arms,[31] and to recognize the different stereoisomers (e.g., D vs L) of polylactide.[32] To probe its ability to measure architectural dispersity, a set of poly(ethylene glycol) (PEG) star polymers were synthesized in a stepwise fashion such that the length of each arm could be tailored with respect to the other arms on the same star polymer.[33] The architectural library of PEG polymers was designed such that the linear PEG control, **1** (~205 repeat units), a 3-arm "mikto"-star, **2**, with arms of different lengths (~18, ~ 49, and ~118 repeat units), and a 4-arm "homo"-star, **3**, with arms of identical length (~49 repeat units), had overlapping mass distributions as apparent in their electrospray ionization (ESI) (Figure 1) and MALDI mass

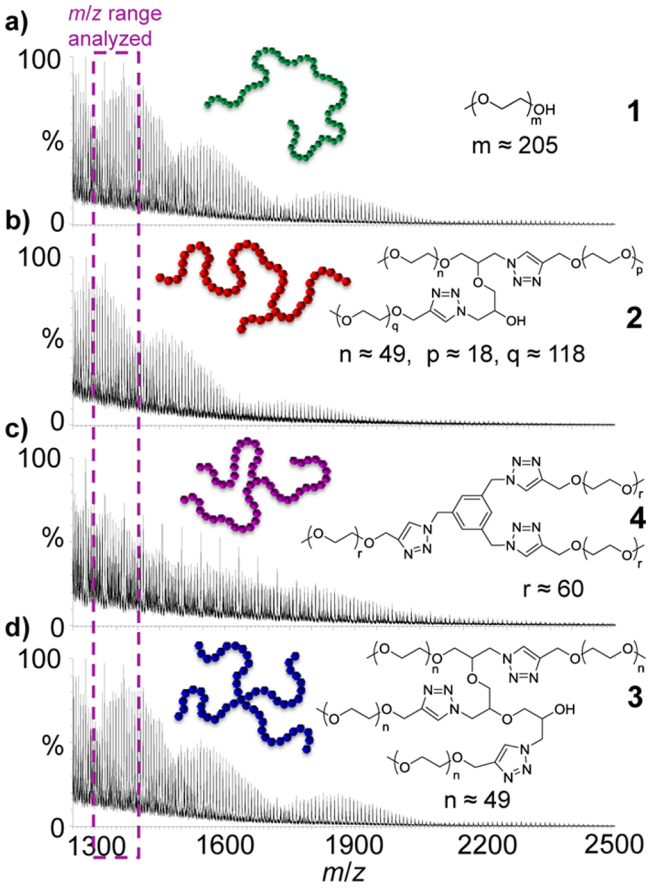

Figure 1. ESI-mass spectra for the synthesized PEG library and their chemical structures: (a) linear PEG, **1**, (b) 3-arm mikto-star, **2**, (c) 3-arm homo-star, **4**, and (d) 4-arm homo-star, **3**. The purple box indicates the portion of the MW distributions that overlapped and were investigated in this study.

spectra (Figure S1, Supporting Information). Using a PEG sample with a broader dispersity, an additional homo-star, **4**, with 3 arms of identical length (~60 repeat units) was also prepared. Insets show the chemical structures and proportional "cartoon" representations of each polymer.

During ESI-IMS-MS experiments, the sample is ionized by association with typically multiple cations forming [polymer + nCat]$^{n+}$ complexes of different sizes that are separated in the TriWave section of the SYNAPT G2. Work by Clemmer offers precedence for improved IMS-MS separation of polymer chains adducting multiple Cs^+ cations.[23,25] Gas-phase ions collide with nitrogen gas as they traverse this region due to motion of a traveling wave. Gas-phase ions that are more extended in their shape experience more collisions and therefore require longer times to reach the detector. Thus, IMS separates ions in the gas phase by "drift time", which is a function of both their collisional cross section, defined by mass and shape, and the number of charges associated with the gas-phase molecular structure.[34] In an IMS-MS experiment, the drift time, m/z, and signal intensity are obtained for each component within a polymer sample giving an information-rich three-dimensional (3-D) plot. For a detailed description of IMS-MS, the reader is referred to literature reviews.[35−37] IMS-MS technology offers promise to successfully identify architectural differences when comparing two synthetic polymers that are structural isomers and, more significantly, to identify architectural dispersity *within* a single sample that is a mixture of different polymer structures.

The rationale for the experimental design and data interpretation is detailed as follows. Charge stabilization can be achieved if the polymer collapses around the cation, providing electron donation from oxygen lone pairs to solvate the cation(s).[23,38,39] When comparing PEG/cation complexes of different MWs, the fewer the charges, the more compact and similar their shapes. On the other hand, with increasing number of charges, the charge−charge repulsion of the metal cations will dominate, stretching the polymer into a more extended conformation.[25] For linear PEG one can expect a more extended structure via charge−charge repulsion at high charge states as compared to branched PEG polymers which are structurally incapable of being as extended. Because different charge states can result in very different gas-phase conformations,[23,25,40] meaningful structural comparisons must be carried out utilizing the same MW range, cation, and charge state. For the library of star polymers evaluated in this study, the +7 charge states with Cs^+ cations generated by ESI were used for comparison in the m/z range between approximately 1350 and 1400 (Figure 1, purple box).

Expanded views of mass spectra (Figures S2 and S3, Supporting Information) and raw data showing relative ion abundances on a false color scale were extracted from two-dimensional (2-D), drift time vs m/z plots (Figures S4−S8, Supporting Information) for each sample analyzed. The corresponding 2-D plots of Figures 2 and 6 (Figures S9−S12) can be found in the Supporting Information along with experimental details.

The IMS drift time measurements of **1**−**3** (those with the narrowest dispersity) exhibit discernible differences that relate to their architectures. For example, the linear PEG sample, expected to exhibit the most extended conformation of the three architectures, exhibited +7 ions with the longest drift time (Figure 2a). On the other extreme, the most compact structure, the 4-arm homo-star +7 ion, exhibited the shortest drift time (Figure 2c). The 3-arm mikto-star +7 ions (Figure 2b) exhibited drift times in between that of the linear and 4-arm star, though much closer to that of linear PEG than the 4-arm star. Thus, the shape of the highly charged gas-phase polymer ion structures followed the trend of decreasing size: linear > 3-arm mikto-star > 4-arm homo-star. The similar drift time of the mikto-star sample **2**, with respect to that of the linear control, **1**, is the result of the relative shortness (~19 repeat units) of the single side chain (the other two arms collectively represent a linear backbone) when contrasted with the two longer (~49 repeat units) pendant chains of the 4-arm homo-star **3**.

Because the 3-D IMS-MS plot includes relative ion abundances for all charge states in the same data set, some of

DOI: 10.1021/acsmacrolett.5b00299
ACS Macro Lett. 2015, 4, 778−782

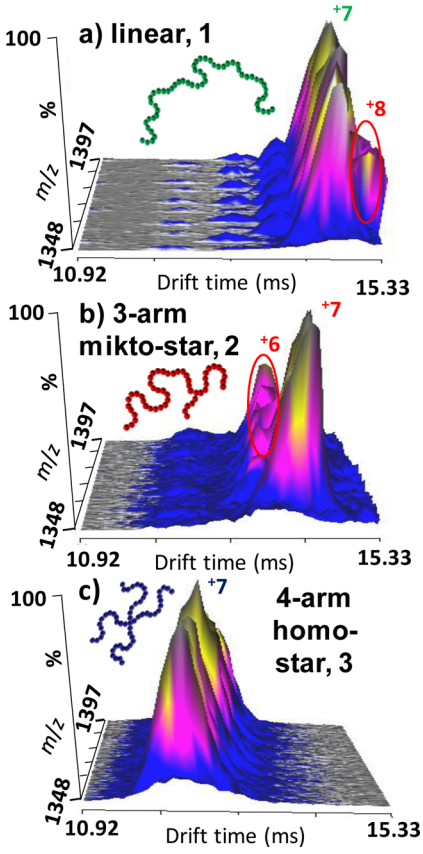

Figure 2. 3-D plot for $[M+7Cs]^{7+}$ samples of M being: (a) linear PEG, **1**, (b) 3-arm mikto-star PEG, **2**, and (c) 4-arm homo-star PEG, **3**. Note: neighboring charge states, linear 8+ and mikto-star 6+, are also observed but can be easily distinguished by different drift times and *m*/*z*'s.

the adjacent charge states (+6 for the 3-arm mikto-star and +8 for the linear) were also apparent. These charge states are easily differentiated in the m/z dimension, as they exhibit a different spacing between *n*-mers as well as within the isotopic distribution. The fact that highly charged polymer ions in the same MW range but differing in architecture exhibit discernible trends in their drift times demonstrates the potential of this tool for elucidating polymer architectures within a few minutes of experimental time. It is important to note that the minor compositional differences, namely, the presence of a different number of triazole linking units (0 for linear, 3 for the 3-arm mitko-star, and 4 for the 4-arm homo-star) or different core structures, will likely result in additional, though minor, deviations in drift times.

It is useful to compare these data to traditional characterization methodologies such as viscometry. As the reciprocal density of the polymer coil in solution, the intrinsic viscosity $[\eta]$ can also reveal aspects of macromolecular architecture. Thus, a graph of $[\eta]$ vs M (Figure 3) confirmed that the linear PEG controls exhibited a predictable trend, illustrated by the Mark–Houwink–Sakurada scaling law ($[\eta] = KM^{\alpha}$). The 3-arm mikto star, **2**, with a structure that deviated only slightly from linear analogues, showed a small offset from this trend observed for the linear controls. However, the 4-arm star, **3**, with a significantly more compact structure and smaller hydrodynamic volume, showed a more substantial deviation from the linear PEG samples.

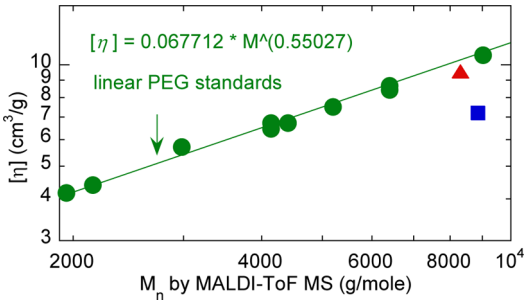

Figure 3. Intrinsic viscosity data for the linear PEG, **1**, M_n = 9030, and other linear PEG standards of various M_n (green, circles), the 3-arm mikto-star PEG, M_n = 8310, **2** (red, triangle), and the 4-arm homo-star PEG (blue, square) M_n = 8860, **3**.

When comparing the viscosity data to the IMS-MS data, the average IMS drift time observed for each *n*-mer within each polymer sample showed a very similar trend (Figure 4), such

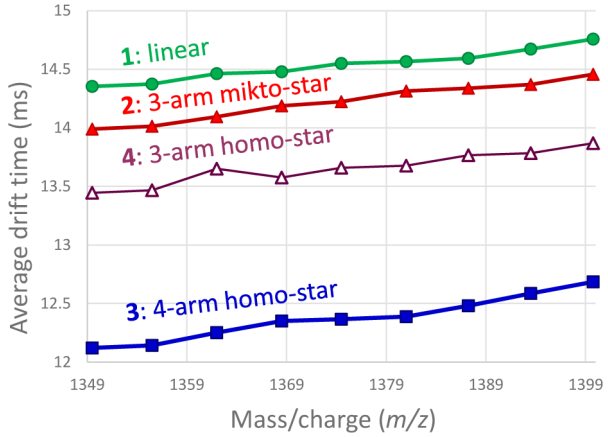

Figure 4. IMS-MS data comparing the average drift times of the $[M+7Cs]^{7+}$ ions for each *n*-mer for the linear PEG, **1** (green, circles), the 3-arm mikto-star PEG, **2** (red, filled triangles), 3-arm homo-star PEG (purple, hollow triangles), **4**, and the 4-arm homo-star PEG (blue, squares), **3**.

that the 3-arm mikto-star PEG (red, filled triangles) was slightly more compact than the linear (green, circles), while the 3-arm homo-star (purple, hollow triangles) was more compact and the 4-arm homo-star PEG the most compact (blue, squares).

However, while viscometry can provide fundamental evidence for the presence of branching, each polymer sample yields only a single data point (an average $[\eta]$ measurement correlated to the number-average molecular weight) complicating the analysis of architectural mixtures. In contrast with the viscometry data, the IMS-MS data are measured for *each* individual *n*-mer component *within* a polymer sample. The value of IMS-MS analysis is especially apparent relative to viscometry when analyzing *mixtures* of different polymer architectures. The intrinsic viscosity of blends with differing proportions of the 4-arm homo-star polymer (**3**) and the linear PEG (**1**) was determined (Figure 5). By tuning the binary mixture to 75% linear and 25% 4-arm star, the measured intrinsic viscosity can mimic that of the 3-arm mikto star.

In contrast, the 3-D IMS-MS plot of this same blend clearly showed the presence of two different polymer architectures within the sample when analyzing the $[M+7Cs]^{7+}$ ions (Figure 6). The differentiation of the two different architectures is also

DOI: 10.1021/acsmacrolett.5b00299
ACS Macro Lett. 2015, 4, 778–782

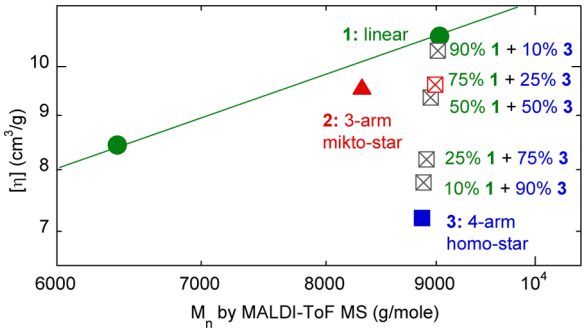

Figure 5. Intrinsic viscosity data comparing the 3-arm mikto-star, **2** (red, triangle), to binary mixtures (crossed squares) of linear, **1** (green, circle), plus 4-arm homo-star (blue, square), **3**. The 75% **1** + 25% **3** mixture exhibits a viscosity nearly identical to that of the 3-arm mikto-star, **2**.

observed for the same mixture in the +6 charge state (Figure S13, Supporting Information).

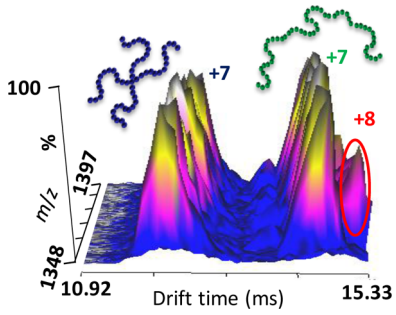

Figure 6. 3-D plot for the $[M+7Cs]^{7+}$ charge state of the mixture exhibits two distinct data trends corresponding to the two architectures present in the blended sample: linear PEG, **1** (right), and 4-arm homo-star PEG, **3** (left).

In summary, IMS-MS has proven to be a powerful technology to distinguish between two samples of similar MW but with different molecular architectures. More significantly, IMS-MS shows great potential in determining architectural dispersity within a sample, a problem where traditional analytical methods have difficulties.[41,42] The strength of this technology lies in the fact that high-resolution separation can be achieved in *both* the drift time *and* m/z dimensions for each component within a polymer sample.

■ ASSOCIATED CONTENT

Supporting Information

All synthetic protocols, characterization methods, and instrumental data. The Supporting Information is available free of charge on the ACS Publications website at DOI: 10.1021/acsmacrolett.5b00299.

■ AUTHOR INFORMATION

Corresponding Authors

*E-mail: sgrayson@tulane.edu
*E-mail: strimpin@chem.wayne.edu.

Notes

The authors declare no competing financial interest.

■ ACKNOWLEDGMENTS

The authors acknowledge support by the National Science Foundation (NSF) under the NSF EPSCoR Cooperative Agreement No. EPS-1430280 with additional support from the Louisiana Board of Regents (BZ, SMG) and NSF CHE 1412439 (AA, SMG). In addition NSF Career Award# 0955975, DuPont Young Professor Award, Waters Center of Innovation Program, and the WSU Rumble Fellowship are acknowledged for support (CDF, ST).

■ REFERENCES

(1) Daoud, M.; Cotton, J. *J. Phys.* **1982**, *43*, 531−538.
(2) Widawski, G.; Rawiso, M.; Francois, B. *Nature* **1994**, *369*, 387−389.
(3) Grest, G. S.; Fetters, L. J.; Huang, J. S.; Richter, D. *Adv. Chem. Phys.* **1996**, *94*, 67−163.
(4) Pakula, T.; Vlassopoulos, D.; Fytas, G.; Roovers, J. *Macromolecules* **1998**, *31*, 8931−8940.
(5) Inoue, K. *Prog. Polym. Sci.* **2000**, *25*, 453−571.
(6) Hedrick, J. L.; Trollsas, M.; Hawker, C. J.; Atthoff, B.; Claesson, H.; Heise, A.; Miller, R. D.; Mecerreyes, D.; Jerome, R.; Dubois, P. *Macromolecules* **1998**, *31*, 8691−8705.
(7) Cloutet, E.; Fillaut, J. L.; Astruc, D.; Gnanou, Y. *Macromolecules* **1998**, *31*, 6748−6755.
(8) Cai, Q.; Zhao, Y. L.; Bei, J. Z.; Xi, F.; Wang, S. G. *Biomacromolecules* **2003**, *4*, 828−834.
(9) Hadjichristidis, N.; Pitsikalis, M.; Pispas, S.; Iatrou, H. *Chem. Rev.* **2001**, *101*, 3747−3792.
(10) Gao, H.; Matyjaszewski, K. *Macromolecules* **2006**, *39*, 4960−4965.
(11) Hoogenboom, R.; Moore, B. C.; Schubert, U. S. *Chem. Commun.* **2006**, *38*, 4010−4012.
(12) Cansell, F.; Botella, P.; Six, J. L.; Garrabos, Y.; Tufeu, R.; Gnanou, Y. *Polym. J.* **1997**, *29*, 910−913.
(13) Li, Y.; Zhang, B.; Hoskins, J. N.; Grayson, S. M. *J. Polym. Sci., Part A: Polym. Chem.* **2012**, *50*, 1086−1101.
(14) Kawaguchi, S.; Imai, G.; Suzuki, J.; Miyahara, A.; Kitano, T. *Polymer* **1997**, *38*, 2885−2891.
(15) Nita, L. E.; Chiriac, A.; Bercea, M.; Wolf, B. A. *Colloids Surf., B* **2013**, *103*, 544−549.
(16) Pfannkoch, E.; Lu, K.; Regnier, F.; Barth, H. *J. Chromatogr. Sci.* **1980**, *18*, 430−441.
(17) Li, Y.; Meunier, D. M.; Partain, E. M. *J. Chromatogr. A* **2014**, *1359*, 182−188.
(18) Rader, H. J.; Schrepp, W. *Acta Polym.* **1998**, *49*, 272−293.
(19) Vidal-de-Miguel, G.; Macia, M.; Barrios, C.; Cuevas, J. *Anal. Chem.* **2015**, *87*, 1925−1932.
(20) Nielen, M. W. F. *Mass Spectrom. Rev.* **1999**, *18*, 309−344.
(21) Koster, S.; Duursma, M. C.; Boon, J. J.; Nielen, M. W.; de Koster, C. G.; Heeren, R. *J. Mass Spectrom.* **2000**, *35*, 739−748.
(22) Nasioudis, A.; Heeren, R. M.; van Doormalen, I.; de Wijs-Rot, N.; van den Brink, O. F. *J. Am. Soc. Mass Spectrom.* **2011**, *22*, 837−844.
(23) Trimpin, S.; Clemmer, D. E. *Anal. Chem.* **2008**, *80*, 9073−9083.
(24) Weidner, S. M.; Trimpin, S. *Anal. Chem.* **2010**, *82*, 4811−4829.
(25) Trimpin, S.; Plasencia, M.; Isailovic, D.; Clemmer, D. E. *Anal. Chem.* **2007**, *79* (21), 7965−7974.
(26) Clemmer, D.; Hudgins, R.; Jarrold, M. *J. Am. Chem. Soc.* **1995**, *117*, 10141−10142.
(27) Koeniger, S. L.; Merenbloom, S. I.; Sevugarajan, S.; Clemmer, D. E. *J. Am. Chem. Soc.* **2006**, *128*, 11713−11719.
(28) Hoskins, J. N.; Trimpin, S.; Grayson, S. M. *Macromolecules* **2011**, *44*, 6915−6918.
(29) Li, X.; Guo, L.; Casiano-Maldonado, M.; Zhang, D.; Wesdemiotis, C. *Macromolecules* **2011**, *44*, 4555−4564.
(30) Josse, T.; De Winter, J.; Dubois, P.; Coulembier, O.; Gerbaux, P.; Memboeuf, A. *Polym. Chem.* **2015**, *6*, 64−69.

DOI: 10.1021/acsmacrolett.5b00299
ACS Macro Lett. 2015, 4, 778−782

(31) Morsa, D.; Defize, T.; Dehareng, D.; Jerome, C.; de Pauw, E. *Anal. Chem.* **2014**, *86*, 9693−9700.
(32) Kim, K.; Lee, J. W.; Chang, T.; Kim, H. I. *J. Am. Soc. Mass Spectrom.* **2014**, *25*, 1771−1779.
(33) Zhang, B.; Zhang, H.; Elupula, R.; Alb, A. M.; Grayson, S. M. *Macromol. Rapid Commun.* **2014**, *35*, 146−151.
(34) Pringle, S. D.; Giles, K.; Wildgoose, J. L.; Williams, J. P.; Slade, S. E.; Thalassinos, K.; Bateman, R. H.; Bowers, M. T.; Scriven, J. H. *Int. J. Mass Spectrom.* **2007**, *261*, 1−12.
(35) Bohrer, B. C.; Merenbloom, S. I.; Koeniger, S. L.; Hilderbrand, A. E.; Clemmer, D. E. *Annu. Rev. Anal. Chem.* **2008**, *1*, 293−10.35327.
(36) May, J. C.; McLean, J. A. *Anal. Chem.* **2015**, *87*, 1422−1436.
(37) Kanu, A. B.; Dwivedi, P.; Tam, M.; Matz, L.; Hill, H. H. J. *J. Mass Spectrom.* **2008**, *43*, 1−22.
(38) Shvartsburg, A. A.; Jarrold, M. F. *Chem. Phys. Lett.* **1996**, *261*, 86−91.
(39) Wyttenbach, T.; von Helden, G.; Bowers, M. T. *Int. J. Mass Spectrom. Ion Processes* **1997**, *165/166*, 377−390.
(40) Larriba, C.; de la Mora, J. F.; Clemmer, D. E. *J. Am. Soc. Mass Spectrom.* **2014**, *25* (8), 1332−1345.
(41) Snijkers, F.; van Ruymbeke, E.; Kim, P.; Lee, H.; Nikopoulou, A.; Chang, T.; Hadjichristidis, N.; Pathak, J.; Vlassopoulos, D. *Macromolecules* **2011**, *44*, 8631−8643.
(42) Van Ruymbeke, E.; Lee, H.; Chang, T.; Nikopoulou, A.; Hadjichristidis, N.; Snijkers, F.; Vlassopoulos, D. *Soft Matter* **2014**, *10*, 4762−4777.

DOI: 10.1021/acsmacrolett.5b00299
ACS Macro Lett. 2015, 4, 778−782